PHYSICAL REVIEW D **93,** 105035 (2016)

Cancellation of infrared divergence in inclusive production of heavy quarkonia

Gao-Liang Zhou

Center for High Energy Physics, Peking University, Beijing 100190, People's Republic of China

(Received 22 December 2015; published 23 May 2016)

A scheme is presented to cancel out topologically unfactorized infrared divergences in the inclusive production of heavy quarkonia, which affect the nonrelativistic QCD (NRQCD) factorization of these processes. Heavy quarkonia are defined as resonance states of QCD instead of a color-singlet heavy quark pair. Thus the final heavy quark pair is not necessarily a color singlet. In addition, heavy quarkonia are reconstructed from their decay products. As a result, the transitions between states containing heavy quarks caused by exchanges of soft gluons are also taken into account here. Such cancellation is crucial for the NRQCD factorization of these processes.

DOI: 10.1103/PhysRevD.93.105035

I. INTRODUCTION

The production of heavy quarkonia forms an important and interesting issue in the study of QCD and the strong interaction [1,2]. The large mass of heavy quarks suggests that one may treat heavy quarkonia as a nonrelativistic bound system. This is supported by quark potential model calculations, which indicate that $v^2 \sim 0.3$ for charmonium and $v^2 \sim 0.1$ for bottomonium [3], where v is the typical velocity in the center-of-mass frame of heavy quarkonia. It has been proposed that the effective theory nonrelativistic QCD (NRQCD) [4,5] could be used to describe the separation of short- and long-distance effects in the production of heavy quarkonia. Short-distance effects that produce a heavy quark pair are perturbative, while long-distance effects that produce the heavy quark pair into heavy quarkonium are nonperturbative and independent of an explicit process. The factorization theorem proposed in Ref. [5] can be written as

$$\mathrm{d}\sigma_{A+B\to H+X} = \sum_n \mathrm{d}\sigma_{A+B\to Q\bar{Q}(n)+X}\langle \mathcal{O}^H(n)\rangle, \qquad (1)$$

where A and B represent initial particles, H represents the detected heavy quarkonium, X represents undetected final particles, and $Q\bar{Q}(n)$ represents the heavy quark pair in a special color and angular momentum state.

Although the NRQCD factorization formula is widely used in the study of the production of heavy quarkonia and has gained great success in the explanation of experimental data (see, for example, Refs. [6–19]), the NRQCD factorization formula still faces challenges, particularly the J/ψ puzzle and the surprisingly large cross section of the associated production of J/ψ in e^+e^-(see, for example, Ref. [1] and references therein). It seems that more efforts are needed to examine the NRQCD factorization formula, especially for inclusive production of heavy quarkonia.

Proofs of the NRQCD factorization theorem for exclusive production of two charmonia in e^+e^- annihilation and the production of a charmonium and a light meson in B-meson decays were established in Refs. [20,21]. For inclusive production of heavy quarkonia, however, the issue is quite nontrivial [22,23]. In Ref. [5], it was argued that infrared divergence caused by exchanges of soft gluons between heavy quarks and extra jets cancel out once the summation over undetected particles has been made, even while one constrains the final heavy quark pair to be a color singlet. According to explicit calculations at next-to-next-to-leading order (NNLO), the authors of Refs. [22,23] found that it is necessary to modify NRQCD octet production matrix elements to include non-Abelian phases (which makes them gauge invariant) in order to restore NRQCD factorization in inclusive production of heavy quarkonia.

In spite of difficulties in the proof of the NRQCD factorization theorem for inclusive production of heavy quarkonia, it was proved [24–28] that collinear factorization holds up to order M^2/p_T^2 for such processes, where M is the mass of the heavy quark and p_T is the transverse momenta of the detected heavy quarkonia in the center-of-mass frame of the initial particles. In the collinear factorization approach, the differential cross section of inclusive production of heavy quarkonium reads

$$\begin{aligned}\mathrm{d}\sigma_{A+B\to H+X} = &\sum_i \mathrm{d}\sigma_{A+B\to i+X} \otimes D_{i\to H} \\ &+ \sum_\kappa \mathrm{d}\sigma_{A+B\to Q\bar{Q}(\kappa)+X} \otimes D_{Q\bar{Q}(\kappa)\to H} \\ &+ \mathcal{O}(M^4/p_T^4), \end{aligned} \qquad (2)$$

where $\mathrm{d}\sigma_{A+B\to i+X}$ represents the differential cross section of inclusive production of a parton i, $D_{i\to H}$ represents the fragmentation function of i into H with i produced in a short-distance process (order $1/p_T$), $\mathrm{d}\sigma_{A+B\to Q\bar{Q}(\kappa)+X}$

represents the differential cross section of inclusive production of a heavy quark pair $Q\bar{Q}$ in a special color and angular momentum state κ, and $D_{Q\bar{Q}(\kappa)\to H}$ represents the fragmentation function of the heavy quark pair $Q\bar{Q}$ into H with the pair produced in a short-distance process (order $1/p_T$). The first term in Eq. (2) contributes from leading power in M/p_T, while the second term contributes from subleading power in M/p_T. If NRQCD factorization holds up to order M^2/p_T^2, then one has [24,26]

$$D_{i\to H} = \sum_n d_{i\to Q\bar{Q}(n)}\langle \mathcal{O}^H(n)\rangle,$$
$$D_{Q\bar{Q}(\kappa)\to H} = \sum_n d_{Q\bar{Q}(\kappa)\to Q\bar{Q}(n)}\langle \mathcal{O}^H(n)\rangle, \tag{3}$$

where $d_{i\to Q\bar{Q}(n)}$ and $d_{Q\bar{Q}(\kappa)\to Q\bar{Q}(n)}$ are short-distance (order $1/M$) coefficients.

In this paper, we present a scheme to cancel out the topologically unfactorized infrared divergences exhibited in Refs. [22,23]. In Refs. [22,23], it was shown that the uncanceled infrared divergences that affect NRQCD factorization originate from diagrams of the type shown in Fig. 1. For an Abelian gauge theory like QED, diagrams of this type do not appear. Thus factorization is not bothered by these diagrams for Abelian gauge theory. One may ask, what happens for non-Abelian gauge theory? For non-Abelian gauge theory, the color of the heavy quark pair is affected by soft gluons which couple to the pair. Once the color state of the final heavy quark pair is fixed, we can no longer make the inclusive summation over all states made up of a heavy quark pair and an arbitrary number of infrared gluons. In fact, the final heavy quark pair is constrained to be color singlet in diagrams of the type shown in Fig. 1. Thus the Kinoshita-Lee-Nauenberg (KLN) cancellation does not simply work in this case. It is necessary to point it out, however, that the color state of the final heavy quark pair is not fixed in the actual process. What we detected were heavy quarkonia like J/ψ, not a color-singlet heavy quark pair in the actual process. Infrared behaviors of higher Fock states should also be taken into account. Summation over these Fock states, however, is not enough to cancel out topologically unfactorized infrared divergences as we will see according to explicit calculations. Exchanges of soft gluons between the heavy quarks and undetected states X may cause a transition between states containing heavy quarks even though the momenta of soft gluons tend to 0! Fortunately, heavy quarkonia are reconstructed from their decay products in actual experiments. As a result, we consider a more inclusive process:

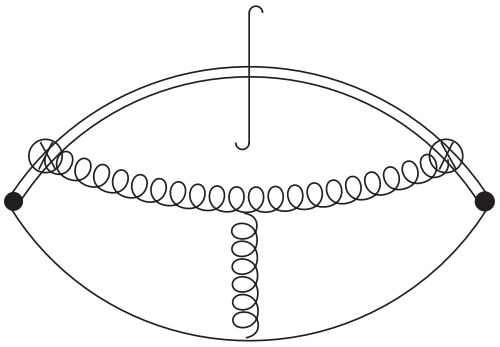

FIG. 1. Topology of diagrams which contribute to uncanceled infrared divergences that affect NRQCD factorization at NNLO. The summation over all cuts that produce a color-singlet heavy quark pair, which is produced as a color octet at the hard vertex, is understood implicitly.

$$A + B \to \mu^+\mu^-(n, p_H) + X, \tag{4}$$

where $\mu^+\mu^-(n, p_H)$ is a $\mu^+\mu^-$ pair with the intrinsic quantum numbers equal to those of the detected heavy quarkonium H. The invariant mass of the $\mu^+\mu^-$ pair is constrained to be near the mass of the heavy quarkonium H. We will show that topologically unfactorized infrared divergences do cancel out in such a process.

The paper is organized as follows. In Sec. II, we describe the inclusive production process of heavy quarkonia. In Sec. III, we take the J/ψ particle as an example to explain how to define heavy quarkonia so that they are invariant under the evolution of infrared QCD interactions. In Sec. IV, we show that summation over higher Fock states is not enough to cancel out topologically unfactorized infrared divergences according to explicit calculations at NNLO. In Sec. V, we consider the inclusive production of a $\mu^+\mu^-$ pair with invariant mass near the mass of a heavy quarkonium H and intrinsic quantum numbers equal to those of H. We show that topologically unfactorized infrared divergences do cancel out in this process. We give our conclusion and some discussions in Sec. VI.

II. INCLUSIVE PRODUCTION OF HEAVY QUARKONIA

In this section, we describe the inclusive production process of heavy quarkonia. The process can be written as

$$A(p_A) + B(p_B) \to H(p_H) + X(p_X), \tag{5}$$

where A and B represent initial particles, and X represents undetected final particles. In the center-of-mass frame of the initial particles, the momenta of A and B are nearly light like. We have

$$p_A^\mu = \bar{n}\cdot p_A n^\mu + n\cdot p_A \bar{n}^\mu \simeq \bar{n}\cdot p_A n^\mu, \tag{6}$$

$$p_B^\mu = n\cdot p_B \bar{n}^\mu + \bar{n}\cdot p_B n^\mu \simeq n\cdot p_B \bar{n}^\mu, \tag{7}$$

where n^μ and $\bar{n}^\mu$ are light-like vectors:

$$n^\mu = \frac{1}{\sqrt{2}}(1,\vec{n}), \qquad \bar{n}^\mu = \frac{1}{\sqrt{2}}(1,-\vec{n}). \tag{8}$$

The transverse momentum of the final heavy quarkonium H is proposed to be much greater than the mass of H. In this case, the momentum of H is also nearly light like in the center-of-mass frame of the initial particles. We have

$$\begin{aligned} p_H^\mu &\equiv \overline{n_H}\cdot p_H n_H^\mu + n_H\cdot p_A \overline{n_H}^\mu \\ &\quad + (p_H^\mu - \overline{n_H}\cdot p_H n_H^\mu + n_H\cdot p_A \overline{n_H}^\mu) \\ &\simeq \overline{n_H}\cdot p_H n_H^\mu, \end{aligned} \tag{9}$$

where n_H^μ and $\overline{n_H}^\mu$ are light-like vectors with

$$n_H^\mu = \frac{1}{\sqrt{2}}(1,\vec{n_H}), \qquad \overline{n_H}^\mu = \frac{1}{\sqrt{2}}(1,-\vec{n_H}). \tag{10}$$

We propose that $n_H\cdot n \sim n_H\cdot \bar{n} \sim 1$ in this paper.

The collinear factorization theorem for the process reads [24–28]

$$\begin{aligned} d\sigma_{A+B\to H+X} &= \sum_i d\sigma_{A+B\to i+X}\otimes D_{i\to H} \\ &\quad + \sum_\kappa d\sigma_{A+B\to c\bar{c}(\kappa)+X}\otimes D_{c\bar{c}(\kappa)\to H} \\ &\quad + \mathcal{O}(M^4/p_T^4), \end{aligned} \tag{11}$$

where the fragmentation functions $D_{i\to H}$ and $D_{c\bar{c}(\kappa)\to H}$ are defined in terms of expectation values of nonlocal operators between vacuumed and final hadron states. For example, the bare fragmentation function of the light quark reads [29]

$$\begin{aligned} D_{q\to H}^{(0)}(z) &= \frac{z^{d-3}}{24\pi}\int dn_H\cdot y e^{-i\overline{n_H}\cdot p_H n_H\cdot y/z} \\ &\quad \times \sum_Y \mathrm{Tr}\langle 0|W_{n_H}^\dagger \psi(0,n_H\cdot y,\vec{0})|HY\rangle \\ &\quad \times \langle HY|\psi^\dagger W_{n_H}(0)|0\rangle, \end{aligned} \tag{12}$$

where z is the ratio of the large momentum component of H to that of the light quark i, and W_{n_H} is the light-like Wilson line,

$$W_{n_H}(x) = \left(\mathcal{P}\exp(ig\int_0^\infty ds\overline{n_H}\cdot A(x+s\overline{n_H})\,)\right)^\dagger. \tag{13}$$

If NRQCD factorization holds up to order M^2/p_T^2, then one has [24,26]

$$\begin{aligned} D_{i\to H} &= \sum_n d_{i\to Q\bar{Q}(n)}\langle \mathcal{O}^H(n)\rangle, \\ D_{Q\bar{Q}(\kappa)\to H} &= \sum_n d_{Q\bar{Q}(\kappa)\to Q\bar{Q}(n)}\langle \mathcal{O}^H(n)\rangle, \end{aligned} \tag{14}$$

where $d_{i\to Q\bar{Q}(n)}$ and $d_{Q\bar{Q}(\kappa)\to Q\bar{Q}(n)}$ are short-distance coefficients. $d_{i\to Q\bar{Q}(n)}$ and $d_{Q\bar{Q}(\kappa)\to Q\bar{Q}(n)}$ should be infrared safe, that is to say, all infrared divergences in $D_{i\to H}$ and $D_{Q\bar{Q}(\kappa)\to H}$ should be absorbed into the long-distance matrix elements of the effective operators $\mathcal{O}^H(n)$. However, calculations in Refs. [22,23] showed that the infrared safety of $d_{i\to Q\bar{Q}(n)}$ and $d_{Q\bar{Q}(\kappa)\to Q\bar{Q}(n)}$ is quite nontrivial once the final detected particle is the color-singlet heavy quark pair.

It is necessary to point out that the final detected particle is H, not the color-singlet heavy quark pair in the process considered here. The color-singlet heavy quark pair is not invariant under the evolution of QCD even though the annihilation of heavy quarks is neglected. The H particle, however, is a stable particle once the decay of H is neglected. Thus, effects of higher Fock states are important in the evolution of heavy quarkonia under infrared QCD interactions.

III. RELATIONS BETWEEN J/ψ AND THE HEAVY QUARK PAIR

In this section, we take the J/ψ particle as an example to show how to define heavy quarkonia so that they are invariant under infrared QCD interactions once the decay of heavy quarkonia is neglected. J/ψ is a stable particle if one neglects the annihilation of the charm quark pair. We thus define the J/ψ state as an eigenstate of NRQCD, where effects of electroweak interactions on the structure of J/ψ are neglected here. We have

$$\vec{P}|J/\psi(j_z,\vec{p})\rangle = \vec{p}|J/\psi(j_z,\vec{p})\rangle, \tag{15}$$

$$J^2|J/\psi(j_z,\vec{0})\rangle = 2|J/\psi(j_z,\vec{0})\rangle, \tag{16}$$

$$J_z|J/\psi(j_z,\vec{0})\rangle = j_z|J/\psi(j_z,\vec{0})\rangle, \tag{17}$$

$$H_{\mathrm{NRQCD}}^{(h)}|J/\psi(j_z,\vec{0})\rangle = (M_{J/\psi}-2M_c)|J/\psi(j_z,\vec{0})\rangle, \tag{18}$$

where $\vec{p}$ represents the momentum of the J/ψ state, j_z represents the z component of the spin of the J/ψ state, $\vec{P}$ and $\vec{J}$ represent the momentum operator and the angular momentum operator, respectively, $M_{J/\psi}$ and M_c represent the mass of J/ψ and the charm quark, respectively, and $H_{\mathrm{NRQCD}}^{(h)}$ represents the Hermitian part of the Hamiltonian of NRQCD. We do not consider the anti-Hermitian part, which describes effects of annihilation of the heavy quark pair, as the width of J/ψ is much smaller than the binding energy of J/ψ.

We expand the J/ψ state according to eigenstates of $H_{\mathrm{NRQCD}}^{(0)}$ which is the free part of H_{NRQCD}; we have

$$|J/\psi(j_z,\vec{0})\rangle = \sum_{m_1,m_2}\int\frac{d^3q}{(2\pi)^3}\phi(\vec{q},j_z,m_1,m_2)|c(\vec{q},m_1)\bar{c}(-\vec{q},m_2)\rangle + \text{high Fock states}, \quad (19)$$

where $|c(\vec{q},m_1)\bar{c}(-\vec{q},m_2)\rangle$ is a color-singlet charm pair, $m_i=\frac{1}{2},-\frac{1}{2}(i=1,\ 2)$, and $\phi(\vec{q},j_z,m_1,m_2)$ is the wave function

$$\phi(\vec{q},j_z,m_1,m_2)=\langle c(\vec{q},m_1)\bar{c}(-\vec{q},m_2)|J/\psi(j_z,\vec{0})\rangle. \quad (20)$$

We bring in the notations

$$|c\bar{c},j_z\rangle_{J/\psi} \equiv \sum_{m_1,m_2}\int\frac{d^3q}{(2\pi)^3}\phi(\vec{q},j_z,m_1,m_2)|c(\vec{q},m_1)\bar{c}(-\vec{q},m_2)\rangle, \quad (21)$$

$$|h,j_z\rangle \equiv |J/\psi(j_z,\vec{0})\rangle - |c\bar{c},\qquad j_z>_{J/\psi}, \quad (22)$$

and then we have

$$|J/\psi(j_z,\vec{0})\rangle = |c\bar{c},j_z\rangle_{J/\psi}+|h,j_z\rangle, \quad (23)$$

$$\langle h,j_z|c\bar{c},j_z\rangle_{J/\psi}=0. \quad (24)$$

The wave function $\phi(\vec{q},j_z,m_1,m_2)$ is nonperturbative, which is treated as an undetermined function in this paper. We assume that the lowest Fock state is the dominate part among the constituents of J/ψ, as was done in Ref. [5]. In terms of perturbation theory, this is equivalent to defining J/ψ as the bound state near the lowest Fock state.

We consider the evolution of the state $|c\bar{c},j_z\rangle_{J/\psi}$:

$$e^{-iH^{(h)}_{\rm NRQCD}t}|c\bar{c},j_z\rangle_{J/\psi} = e^{-i(M_{J/\psi}-2M_c)t}\langle J/\psi(j_z,\vec{0})|c\bar{c},j_z\rangle_{J/\psi}|J/\psi(j_z,\vec{0})\rangle + \sum_{n=2}^{\infty}e^{-iE_nt}\langle n,j_z,\vec{0}|c\bar{c},j_z\rangle_{J/\psi}|n,j_z,\vec{0}\rangle, \quad (25)$$

where $|n\rangle$ represents the spin-one eigenstate of $H^{(h)}_{\rm NRQCD}$ that contains a heavy quark pair. J/ψ is the state with the smallest invariant mass among these states, and we thus have

$$E_n > M_{J/\psi}-2M_c(n\geq 2). \quad (26)$$

We then have

$$\lim_{t\to\infty(1-i\epsilon)}e^{-i(H^{(h)}_{\rm NRQCD}-M_{J/\psi}+2M_c)t}|c\bar{c},j_z\rangle_{J/\psi} = \langle J/\psi(j_z,\vec{0})|c\bar{c},j_z\rangle_{J/\psi}|J/\psi(j_z,\vec{0})\rangle. \quad (27)$$

We thus define the J/ψ state as

$$|J/\psi(j_z,\vec{0})\rangle = \frac{1}{\langle J/\psi(j_z,\vec{0})|c\bar{c},j_z\rangle_{J/\psi}} \times\lim_{t\to\infty(1-i\epsilon)}e^{-i(H^{(h)}_{\rm NRQCD}-M_{J/\psi}+2M_c)t}|c\bar{c},j_z\rangle_{J/\psi}. \quad (28)$$

According to Eqs. (21) and (20), we have

$$\langle J/\psi(j_z,\vec{0})|c\bar{c},j_z\rangle_{J/\psi} = \sum_{m_1,m_2}\int\frac{d^3q}{(2\pi)^3}|^2\phi(\vec{q},j_z,m_1,m_2)| = \sum_{m_1,m_2}\int\frac{d^3q}{(2\pi)^3}|\langle c(\vec{q},m_1)\bar{c}(-\vec{q},m_2)|J/\psi(j_z,\vec{0})\rangle|^2. \quad (29)$$

The undetermined parameter $\langle J/\psi(j_z,\vec{0})|c\bar{c},j_z\rangle_{J/\psi}$ is independent of the Fock states in the perturbation series. It can be dropped in the following calculations.

According to Eqs. (21) and (28), we have

$$\begin{aligned}|J/\psi(j_z,\vec{0})\rangle &= \frac{1}{\langle J/\psi(j_z,\vec{0})|c\bar{c},j_z\rangle_{J/\psi}}\sum_{m_1,m_2}\int\frac{d^3q}{(2\pi)^3}\phi(\vec{q},j_z,m_1,m_2)\lim_{t\to\infty(1-i\epsilon)}e^{-iH^{(0)}_{\rm NRQCD}t}e^{iH^{(0)}_{\rm NRQCD}t}\\ &\quad\times e^{-i(H^{(h)}_{\rm NRQCD}-M_{J/\psi}+2M_c)t}|c(\vec{q},m_1)\bar{c}(-\vec{q},m_2)\rangle\\ &= \frac{1}{\langle J/\psi(j_z,\vec{0})|c\bar{c},j_z\rangle_{J/\psi}}\sum_{m_1,m_2}\int\frac{d^3q}{(2\pi)^3}\phi(\vec{q},j_z,m_1,m_2)\lim_{t\to\infty(1-i\epsilon)}e^{-i(H^{(0)}_{\rm NRQCD}-M_{J/\psi}+2M_c)t}\\ &\quad\times\left(T\left\{\exp\left(-i\int_0^t dt' H^{(I)}_{\rm NRQCD}(t')\right)\right\}\right)|c(\vec{q},m_1)\bar{c}(-\vec{q},m_2)\rangle, \end{aligned} \quad (30)$$

where $H^{(0)}_{\mathrm{NRQCD}}$ is the free part of H_{NRQCD}, E_q is the energy of the charm quark with momentum $\vec{q}$,

$$E_q = \sqrt{M_c^2 + |\vec{q}|^2}, \tag{31}$$

and $H^{(I)}_{\mathrm{NRQCD}}(t')$ is defined as

$$H^{(I)}_{\mathrm{NRQCD}}(t') = e^{iH^{(0)}_{\mathrm{NRQCD}}t'}(H^{(h)}_{\mathrm{NRQCD}} - H^{(0)}_{\mathrm{NRQCD}})e^{-iH^{(0)}_{\mathrm{NRQCD}}t'}. \tag{32}$$

We notice that the $i\epsilon$ term in Eq. (30) is in accordance with the Feynman boundary conditions. We can thus calculate the perturbation series of Eq. (30) according to Feynman diagram skills.

IV. CONTRIBUTIONS OF HIGHER FOCK STATES

In this section, we consider contributions of higher Fock states of the J/ψ particle in fragmentation functions $D_{i\to J/\psi}$ and $D_{c\bar{c}(\kappa)\to J/\psi}$ up to NNLO.

The term $e^{-i(H^{(0)}_{\mathrm{NRQCD}}-M_{J/\psi}+2M_c)t}$ is independent of Fock states once the relative momenta of the final heavy quark pair is definite in the infrared limit. We thus simply drop this term in the following calculations. To determine infrared divergences caused by soft gluons exchanged between J/ψ and other energetic particles, we take the eikonal line approximation in couplings of soft gluons to the on-shell charm quark pair. This is equivalent to absorbing effects of these soft gluons into Wilson lines:

$$Y_v(0) = \mathcal{P}\exp\left(-ig\int_0^\infty \mathrm{d}sv\cdot A(sv)\right), \tag{33}$$

where

$$v^\mu = \frac{p^\mu}{2p^0}, \tag{34}$$

where p^μ are the momenta of final heavy quarks.

The gauge-invariant effective operators defined in Refs. [22,23] read

$$\mathcal{O} = \sum_{X,j_z}\chi^\dagger Y_l^\dagger(0)\mathcal{K}Y_l(0)\psi(0)|J/\psi(j_z,\vec{0})X\rangle \times\langle J/\psi(j_z,\vec{0})X|\psi^\dagger Y_l^\dagger(0)\mathcal{K}'Y_l(0)\chi(0), \tag{35}$$

where ψ is the Pauli spinor field that annihilates the charm quark, χ is the Pauli spinor field that creates the anticharm quark, and $\mathcal{K}$ and $\mathcal{K}'$ are possible color, spin, and covariant derivative terms. We consider the evolution of a color octet charm pair to the J/ψ state. The infrared behavior of this evolution can be written as

$$\mathcal{O}^{(8)}(v_1,v_2;v_1',v_2') = \sum_X\langle 0|(Y^\dagger_{v_2}t^aY_{v_1})_{ij}Y_l^\dagger(0)_{ac}|J/\psi X\rangle \times\langle J/\psi X|Y_l(0)_{cb}(Y^\dagger_{v_2'}t^bY_{v_1'})^\dagger_{kl}|0\rangle, \tag{36}$$

where v_1 and v_1' are velocities of final charm quarks, and v_2 and v_2' are velocities of final anticharm quarks. $v_i \neq v_i'(i=1,2)$ in general. We do not require that $i=j$ or $k=l$ as the final charm quark pair can be a color octet.

Examples of diagrams—of which the lowest Fock states in Eq. (30) are produced by the evolution of the color-octet heavy quark pair—are shown in Fig. 2. In Fig. 2, we take the same value for the relative momenta of the charm pair on both sides of the final cuts, as in Refs. [22,23]. If we neglect the term $\lim_{t\to\infty(1-i\epsilon)}e^{-i(2E_q-M_{J/\psi}+2M_c)t}$, which does not affect the cancellation of infrared divergences, then the topologically unfactorized infrared divergent part of the summation of these diagrams reads [22,23]

$$\epsilon^{(8\to1)}(c\bar{c}) = -\frac{N_c}{4}(N_c^2-1)\frac{\alpha_s^2}{4\epsilon}\left[1-\frac{1}{f(|\vec{v}|)}\ln\left(\frac{1+f(|\vec{v}|)}{1-f(|\vec{v}|)}\right)\right] + O(\alpha_s^3), \tag{37}$$

$$f(x) = \frac{2x}{1+x^2}, \tag{38}$$

where $\vec{v}$ is the relative velocity of the heavy quark in the center-of-mass frame of the heavy quark pair.

Except for the lowest Fock state, the Fock state $|c\bar{c}g\rangle$ in Eq. (30) also contributes to the cross section up to NNLO in QCD interactions. Diagrams with higher Fock states take

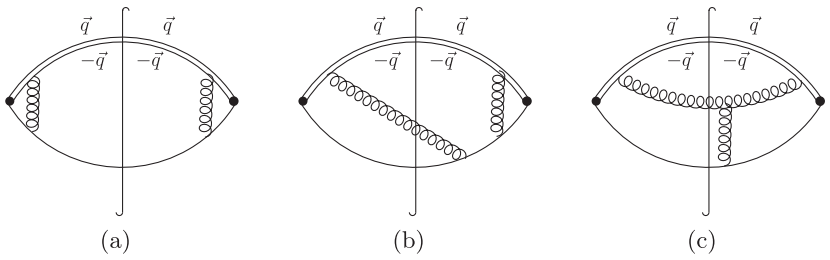

FIG. 2. Examples of diagrams where a color-singlet $c\bar{c}$ pair is produced by the evolution of a color-octet $c\bar{c}$ pair.

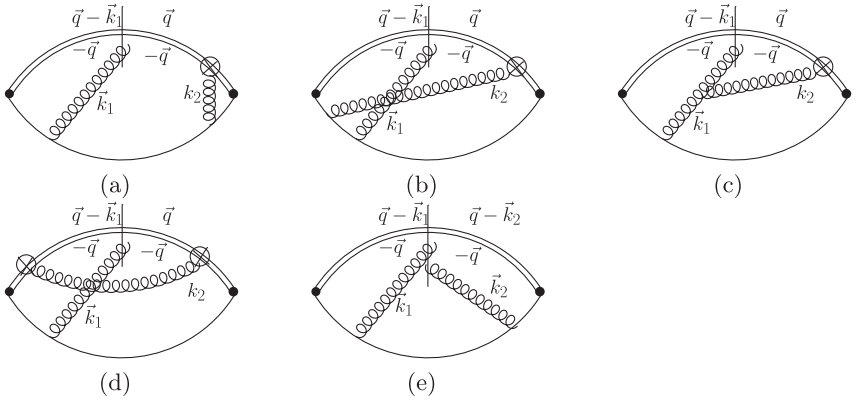

FIG. 3. Diagrams with the Fock states $|c\bar{c}g\rangle$ in the final states.

the forms shown in Fig. 3 or their conjugations, where the effective vertex $\otimes$ is defined in Fig. 4. Color factors of the first and the last diagram in Fig. 3 read

$$C^{3a} \propto \mathrm{tr}[t^a t^b] f^{abc} = 0,$$
$$C^{3e} \propto \mathrm{tr}[t^a t^b]\mathrm{tr}[t^d t^e] f^{abc} f^{cde} = 0. \tag{39}$$

In the following, we thus neglect these diagrams and discuss the remaining diagrams explicitly. Without loss of generality, we take l^μ to be

$$l^\mu = \frac{1}{\sqrt{2}}(1,0,0,1) \tag{40}$$

in the following calculations. The difference between these diagrams and those in Fig. 2 is that real gluons in Fig. 2 belong to the undetected state X, while the real gluon k_1 in Fig. 3 belongs to the constituents of the detected J/ψ particle.

A. Diagrams that take the form shown in Fig. 3(b)

In this subsection, we consider the diagrams shown in Fig. 5.

For the first diagram in Fig. 5, we have

$$\Sigma^{5a}(j) = \int \frac{\mathrm{d}^{D-1}k_1}{(2\pi)^{D-1}2|\vec{k}_1|}\int \frac{\mathrm{d}^{D-1}k_2}{(2\pi)^{D-1}2|\vec{k}_2|} N^{5a}(j)\frac{1}{l\cdot k_1 + i\epsilon} \times \frac{1}{l\cdot(k_1+k_2)+i\epsilon}\frac{1}{v_1\cdot k_1 - i\epsilon}\frac{1}{v_j\cdot k_2 - i\epsilon}\Big|_{\{k_1^0=|\vec{k}_1|,k_2^0=|\vec{k}_2|\}}, \tag{41}$$

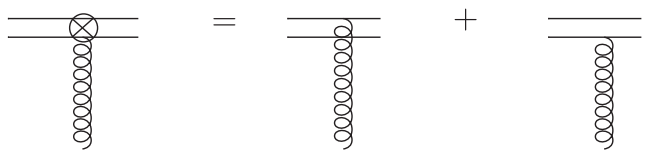

FIG. 4. Definition of the vertex $\otimes$ in Fig. 3.

where $j = 1, 2$, and the numerator term $N^{5a}(j)$ reads

$$N^{5a}(j) = \begin{cases} g^4\mu^{4\epsilon} l\cdot v_1 l\cdot v_1 N_c(N_c^2-1)/4 & \text{for } j=1, \\ -g^4\mu^{4\epsilon} l\cdot v_1 l\cdot v_2 N_c(N_c^2-1)/4 & \text{for } j=2. \end{cases} \tag{42}$$

For the second diagram in Fig. 5, we have

$$\Sigma^{5b}(j) = \int \frac{\mathrm{d}^{D-1}k_1}{(2\pi)^{D-1}2|\vec{k}_1|}\int \frac{\mathrm{d}^{D-1}k_2}{(2\pi)^{D-1}2|\vec{k}_2|} N^{5b}(j) \times \frac{1}{l\cdot k_1 + i\epsilon}\frac{1}{l\cdot(k_1+k_2)+i\epsilon}\frac{1}{v_2\cdot k_1 - i\epsilon} \times \frac{1}{v_j\cdot k_2 - i\epsilon}\Big|_{\{k_1^0=|\vec{k}_1|,k_2^0=|\vec{k}_2|\}}, \tag{43}$$

where $j = 1, 2$, and the numerator term $N^{5a}(j)$ reads

$$N^{5b}(j) = \begin{cases} -g^4\mu^{4\epsilon} l\cdot v_2 l\cdot v_1 N_c(N_c^2-1)/4 & \text{for } j=1, \\ g^4\mu^{4\epsilon} l\cdot v_2 l\cdot v_2 N_c(N_c^2-1)/4 & \text{for } j=2. \end{cases} \tag{44}$$

The summation of these diagrams reads

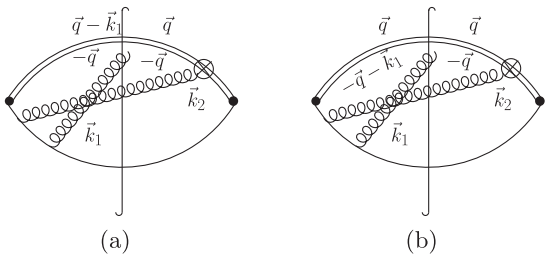

FIG. 5. Diagrams that take the form shown in Fig. 3(b).

$$\sum_{j=1}^{2}(\Sigma^{5a}(j)+\Sigma^{5b}(j)) = g^4\mu^{4\epsilon}\frac{N_c(N_c^2-1)}{4}\int\frac{\mathrm{d}^{D-1}k_1}{(2\pi)^{D-1}2|\vec{k}_1|}\int\frac{\mathrm{d}^{D-1}k_2}{(2\pi)^{D-1}2|\vec{k}_2|}\frac{1}{l\cdot k_1+i\epsilon} \times\frac{1}{l\cdot(k_1+k_2)+i\epsilon}\left(\frac{l\cdot v_1}{v_1\cdot k_1-i\epsilon}-\frac{l\cdot v_2}{v_2\cdot k_1-i\epsilon}\right)\left(\frac{l\cdot v_1}{v_1\cdot k_2-i\epsilon}-\frac{l\cdot v_2}{v_2\cdot k_2-i\epsilon}\right)\Big|_{\{k_1^0=|\vec{k}_1|,k_2^0=|\vec{k}_2|\}}. \tag{45}$$

If k_1 or k_2 is collinear to l^μ, then we have

$$v_i\cdot k_j = v_i^- k_j^+, \tag{46}$$

where $i=1,2$, $j=1,2$. One can verify that contributions of these regions cancel out between the diagrams shown in Fig. 5. We thus do not consider the collinear divergences of these diagrams here.

We have

$$\begin{aligned}\sum_{j=1}^{2}(\Sigma^{5a}(j)+\Sigma^{5b}(j)) &= g^4\mu^{4\epsilon}\frac{N_c(N_c^2-1)}{4}\int\frac{\mathrm{d}^{D-2}k_{1\perp}}{(2\pi)^{D-2}}\int\frac{\mathrm{d}^{D-2}k_{2\perp}}{(2\pi)^{D-2}}\int_0^\infty\frac{\mathrm{d}k_1^-}{2\pi}\int_0^\infty\frac{\mathrm{d}k_2^-}{2\pi}\\ &\times\frac{1}{k_1^-+i\epsilon}\frac{1}{k_1^-+k_2^-+i\epsilon}\left(\frac{v_1^-}{2v_1^+(k_1^-)^2+v_1^-k_{1\perp}^2-2k_1^-v_{1\perp}\cdot k_{1\perp}-i\epsilon}\right.\\ &\left.-\frac{v_2^-}{2v_2^+(k_1^-)^2+v_2^-k_{1\perp}^2-2k_1^-v_{2\perp}\cdot k_{1\perp}-i\epsilon}\right)\left(\frac{v_1^-}{2v_1^+(k_2^-)^2+v_1^-k_{2\perp}^2-2k_1^-v_{1\perp}\cdot k_{2\perp}-i\epsilon}\right.\\ &\left.-\frac{v_2^-}{2v_2^+(k_2^-)^2+v_2^-k_{2\perp}^2-2k_1^-v_{2\perp}\cdot k_{2\perp}-i\epsilon}\right)\\ &= \frac{\alpha_s^2}{32\pi^2}\frac{N_c(N_c^2-1)}{4}\left(\frac{1}{\epsilon}\right)^2\left[\ln^2\frac{(v_1\cdot l)^2}{(v_2\cdot l)^2}-2\epsilon\ln\frac{\Lambda^2}{\mu^2}\ln^2\frac{(v_1\cdot l)^2}{(v_2\cdot l)^2}\right.\\ &\left.+\epsilon\left(\ln^2\frac{(v_1\cdot l)^2}{(v_1)^2}-\ln^2\frac{(v_2\cdot l)^2}{(v_2)^2}\right)\ln\frac{(v_1\cdot l)^2}{(v_2\cdot l)^2}\right]+(\text{infrared safe terms}),\end{aligned} \tag{47}$$

where Λ is the parameter chosen to regularize ultraviolet divergences.

For conjugations of diagrams in Fig. 5, we have the same result; that is,

$$\begin{aligned}(\text{Fig. 5}+\text{conjugations}) &= \frac{\alpha_s^2}{16\pi^2}\frac{N_c(N_c^2-1)}{4}\left(\frac{1}{\epsilon}\right)^2\left[\ln^2\frac{(v_1\cdot l)^2}{(v_2\cdot l)^2}-2\epsilon\ln\frac{\Lambda^2}{\mu^2}\ln^2\frac{(v_1\cdot l)^2}{(v_2\cdot l)^2}\right.\\ &\left.+\epsilon\left(\ln^2\frac{(v_1\cdot l)^2}{(v_1)^2}-\ln^2\frac{(v_2\cdot l)^2}{(v_2)^2}\right)\ln\frac{(v_1\cdot l)^2}{(v_2\cdot l)^2}\right]+(\text{infrared-safe terms}).\end{aligned} \tag{48}$$

B. Diagrams that take the form shown in Fig. 3(c)

In this subsection, we consider the diagrams shown in Fig. 6.

For the first diagram in Fig. 6, we have

$$\Sigma^{6a}(j) = \int\frac{\mathrm{d}^{D-1}k_1}{(2\pi)^{D-1}2|\vec{k}_1|}\int\frac{\mathrm{d}^{D-1}k_2}{(2\pi)^{D-1}2|\vec{k}_2|}N^{6a}(k_1,k_2,j)\frac{1}{(k_1+k_2)^2+i\epsilon} \times\frac{1}{l\cdot(k_1+k_2)+i\epsilon}\frac{1}{v_1\cdot k_1-i\epsilon}\frac{1}{v_j\cdot k_2-i\epsilon}\Big|_{\{k_1^0=|\vec{k}_1|,k_2^0=|\vec{k}_2|\}}, \tag{49}$$

where $j=1,2$, and the numerator term $N^{6a}(j)$ reads

$$N^{6a}(k_1,k_2,j)=\begin{cases}\frac{g^4\mu^{4\epsilon}}{4}N_c(N_c^2-1)[v_1\cdot lv_1\cdot(-2k_1-k_2)+v_1\cdot lv_1\cdot(k_1+2k_2)+v_1\cdot v_1 l\cdot(k_1-k_2)] & \text{for } j=1,\\ -\frac{g^4\mu^{4\epsilon}}{4}N_c(N_c^2-1)[v_1\cdot lv_2\cdot(-2k_1-k_2)+v_2\cdot lv_1\cdot(k_1+2k_2)+v_1\cdot v_2 l\cdot(k_1-k_2)] & \text{for } j=2.\end{cases} \tag{50}$$

For the second diagram in Fig. 6, we have

$$\Sigma^{6b}(j)=\int\frac{\mathrm{d}^{D-1}k_1}{(2\pi)^{D-1}2|\vec{k}_1|}\int\frac{\mathrm{d}^{D-1}k_2}{(2\pi)^{D-1}2|\vec{k}_2|}N^{6b}(k_1,k_2,j)\frac{1}{(k_1+k_2)^2+i\epsilon}\times\frac{1}{l\cdot(k_1+k_2)+i\epsilon}\frac{1}{v_2\cdot k_1-i\epsilon}\frac{1}{v_j\cdot k_2-i\epsilon}\Big|_{\{k_1^0=|\vec{k}_1|,k_2^0=|\vec{k}_2|\}}, \tag{51}$$

where $j=1,2$, and the numerator term $N^{6b}(j)$ reads

$$N^{6b}(k_1,k_2,j)=\begin{cases}-\frac{g^4\mu^{4\epsilon}}{4}N_c(N_c^2-1)[v_2\cdot lv_1\cdot(-2k_1-k_2)+v_1\cdot lv_2\cdot(k_1+2k_2)+v_2\cdot v_1 l\cdot(k_1-k_2)] & \text{for } j=1,\\ \frac{g^4\mu^{4\epsilon}}{4}N_c(N_c^2-1)[v_2\cdot lv_2\cdot(-2k_1-k_2)+v_2\cdot lv_2\cdot(k_1+2k_2)+v_2\cdot v_2 l\cdot(k_1-k_2)] & \text{for } j=2.\end{cases} \tag{52}$$

We first consider contributions of collinear regions. Contributions from the region where $k_1(k_2)$ is collinear to l^μ and $l\cdot k_2(l\cdot k_1)$ is finite are power suppressed. In the region where $k_1(k_2)$ is collinear to l^μ and $k_2(k_1)$ is infrared, we have

$$v_1\cdot k_1=v_1^-k_1^+,\qquad M^{6a}(k_1,k_2,j)=M^{6a}(\tilde{k}_1,0,j) \tag{53}$$

or

$$v_j\cdot k_2=v_j^-k_2^+,\qquad M^{6a}(k_1,k_2,j)=M^{6a}(0,\tilde{k}_2,j), \tag{54}$$

where

$$(\tilde{k}_1^+,\tilde{k}_1^-,\vec{\tilde{k}}_{1\perp})=(k_1^+,0,\vec{0}), \tag{55}$$

$$(\tilde{k}_2^+,\tilde{k}_2^-,\vec{\tilde{k}}_{2\perp})=(k_2^+,0,\vec{0}). \tag{56}$$

One can verify that contributions from these regions cancel out between the diagrams shown in Fig. 6. If both k_1 and k_2 are collinear to l^μ, then we have

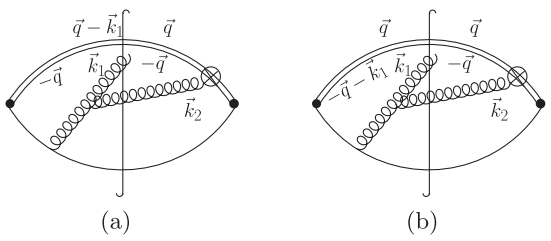

FIG. 6. Diagrams that take the form shown in Fig. 3(c).

$$v_1\cdot k_1=v_1^-k_1^+,\qquad v_j\cdot k_2=v_j^-k_2^+. \tag{57}$$

Contributions from such regions cancel out between $\Sigma^{6a}(1)$ and $\Sigma^{6a}(2)$. If k_1 is collinear to k_2 with $l\cdot k_1$ and $l\cdot k_2$ finite, then we have

$$v_1\cdot k_1\propto v_1\cdot k_2,\quad v_j\cdot k_1\propto v_2\cdot k_2,\quad l\cdot k_1\propto l\cdot k_2. \tag{58}$$

Contributions from such regions also cancel out between $\Sigma^{6a}(1)$ and $\Sigma^{6a}(2)$. Thus collinear divergences do not disturb us.

The summation of $\Sigma^{6a}(j)$ and $\Sigma^{6b}(j)$ vanishes as integrands are antisymmetric under the exchange $\vec{k}_1\leftrightarrow\vec{k}_2$. We see that infrared-divergent terms in the diagrams shown in Fig. 6 cancel out. We have

$$\text{Fig. 6}=(\text{Fig. 6})^*=0. \tag{59}$$

C. Diagrams that take the form shown in Fig. 3(d)

In this subsection, we consider the diagrams shown in Fig. 7. For the first diagram in Fig. 7, we have

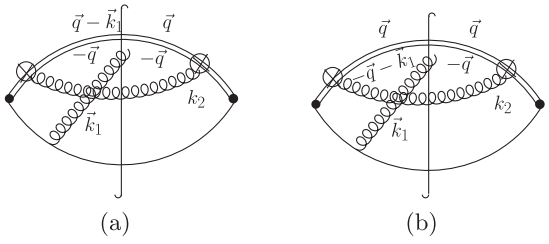

FIG. 7. Diagrams that take the form shown in Fig. 3(d).

$$\Sigma^{7a}(j,j') = \int \frac{\mathrm{d}^{D-1}k_1}{(2\pi)^{D-1}2|\vec{k}_1|}\int \frac{\mathrm{d}^{D-1}k_2}{(2\pi)^{D-1}2|\vec{k}_2|} N^{7a}(j,j')\frac{1}{l\cdot k_1 + i\epsilon}\frac{1}{v_1\cdot k_1 - i\epsilon}\frac{1}{v_j\cdot k_2 + i\epsilon}\frac{1}{v_{j'}\cdot k_2 - i\epsilon}\Big|_{\{k_1^0=|\vec{k}_1|,k_2^0=|\vec{k}_2|\}}, \tag{60}$$

where $j = 1, 2$, $j' = 1, 2$, and the numerator term $N^{6a}(j,j')$ is defined as

$$N^{7a}(j,j') = \begin{cases} -\frac{g^4\mu^{4\epsilon}}{8}N_c(N_c^2-1)v_1\cdot v_1 l\cdot v_1 & \text{for } j=j'=1, \\ \frac{g^4\mu^{4\epsilon}}{8}N_c(N_c^2-1)v_1\cdot v_2 l\cdot v_1 & \text{for } j=1, j'=2, \\ -\frac{g^4\mu^{4\epsilon}}{8}N_c(N_c^2-1)v_1\cdot v_2 l\cdot v_1 & \text{for } j=2, j'=1, \\ \frac{g^4\mu^{4\epsilon}}{8}N_c(N_c^2-1)v_2\cdot v_2 l\cdot v_1 & \text{for } j=j'=2. \end{cases} \tag{61}$$

For the second diagram in Fig. 7, we have

$$\Sigma^{7b}(j,j') = \int \frac{\mathrm{d}^{D-1}k_1}{(2\pi)^{D-1}2|\vec{k}_1|}\int \frac{\mathrm{d}^{D-1}k_2}{(2\pi)^{D-1}2|\vec{k}_2|} N^{7b}(j,j')\frac{1}{l\cdot k_1 + i\epsilon}\frac{1}{v_2\cdot k_1 - i\epsilon}\frac{1}{v_j\cdot k_2 + i\epsilon}\frac{1}{v_{j'}\cdot k_2 - i\epsilon}\Big|_{\{k_1^0=|\vec{k}_1|,k_2^0=|\vec{k}_2|\}}, \tag{62}$$

where $j = 1, 2$, $j' = 1, 2$, and the numerator term $N^{6a}(j,j')$ is defined as

$$N^{7b}(j,j') = \begin{cases} \frac{g^4\mu^{4\epsilon}}{8}N_c(N_c^2-1)v_1\cdot v_1 l\cdot v_2 & \text{for } j=j'=1, \\ -\frac{g^4\mu^{4\epsilon}}{8}N_c(N_c^2-1)v_1\cdot v_2 l\cdot v_2 & \text{for } j=1, j'=2, \\ \frac{g^4\mu^{4\epsilon}}{8}N_c(N_c^2-1)v_1\cdot v_2 l\cdot v_2 & \text{for } j=2, j'=1, \\ -\frac{g^4\mu^{4\epsilon}}{8}N_c(N_c^2-1)v_2\cdot v_2 l\cdot v_2 & \text{for } j=j'=2. \end{cases} \tag{63}$$

If k_1 is collinear to l^μ, then we have

$$v_1\cdot k_1 \simeq v_1^- l_1^+, \qquad v_2\cdot k_1 \simeq v_2^- k_2^+. \tag{64}$$

Contributions from such regions cancel out between $\Sigma^{7a}(j,j')$ and $\Sigma^{7b}(j,j')$. We thus do not consider effects of collinear divergences.

We see that

$$\sum_{j,j'}(\Sigma^{7a}(j,j') + \Sigma^{7b}(j,j')) = 0, \tag{65}$$

as integrands are antisymmetric under the transformation $\vec{k}_2 \to -\vec{k}_2$. Thus infrared-divergent terms in the diagrams shown in Fig. 7 cancel out. We have

$$\text{Fig.7} = (\text{Fig.7})^* = 0. \tag{66}$$

According to Eqs. (48), (59), and (66), we have

$$\begin{aligned}\epsilon^{(8\to1)}(\text{high Fock states}) = {}& \frac{\alpha_s^2}{16\pi^2}\frac{N_c(N_c^2-1)}{4}\left(\frac{1}{\varepsilon}\right)^2\left[\ln^2\frac{(v_1\cdot l)^2}{(v_2\cdot l)^2} - 2\varepsilon\ln\frac{\Lambda^2}{\mu^2}\ln^2\frac{(v_1\cdot l)^2}{(v_2\cdot l)^2}\right. \\ & \left. + \varepsilon\left(\ln^2\frac{(v_1\cdot l)^2}{(v_1)^2} - \ln^2\frac{(v_2\cdot l)^2}{(v_2)^2}\right)\ln\frac{(v_1\cdot l)^2}{(v_2\cdot l)^2}\right] + (\text{infrared safe terms}) + O(\alpha_s^3).\end{aligned} \tag{67}$$

We see that the summation of Eqs. (37) and (67) is not infrared safe. In particular, infrared-divergent terms in Eq. (37) are of order $\frac{1}{\varepsilon}$, while those in Eq. (67) are of order $\frac{1}{\varepsilon^2}$ or $\frac{1}{\varepsilon}$. We conclude that fragmentation functions $D_{i\to J/\psi}$ and $D_{c\bar{c}(\kappa)\to J/\psi}$ suffer from topologically unfactorized infrared divergences shown in Eq. (37) even when contributions of higher Fock states are taken into account.

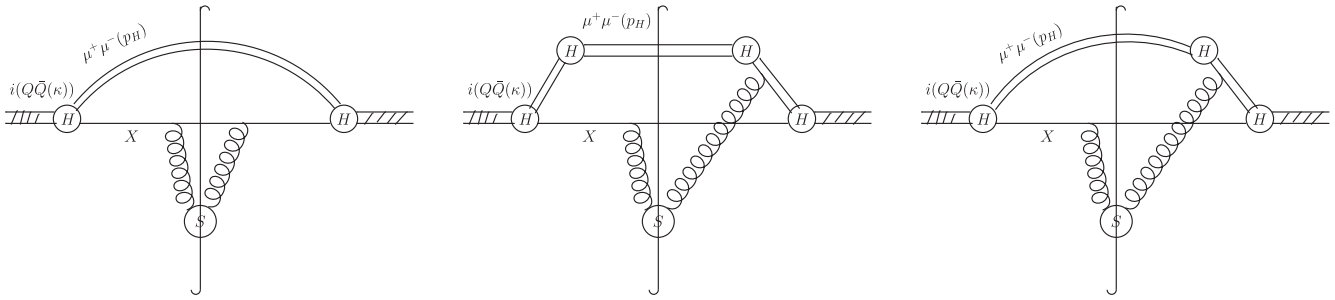

FIG. 8. (a) Example of direct production of $\mu^+\mu^-$ pair in fragmentation functions $D_{i\to\mu^+\mu^-(n,p_H)}$ and $D_{Q\bar{Q}(\kappa)\to\mu^+\mu^-(n,p_H)}$. (b) Example of indirect production of $\mu^+\mu^-$ pair in fragmentation functions $D_{i\to\mu^+\mu^-(n,p_H)}$ and $D_{Q\bar{Q}(\kappa)\to\mu^+\mu^-(n,p_H)}$. (c) Example of interference terms between the direct and indirect production of a $\mu^+\mu^-$ pair.

V. INCLUSIVE PRODUCTION OF STABLE PARTICLES NEAR THE THRESHOLD OF HEAVY QUARKONIA

In a practical process, detected heavy quarkonia are reconstructed from their decay products. Without loss of generality, we consider the process

$$A + B \to \mu^+\mu^-(n, p_H) + X \tag{68}$$

in this section, where A and B represent initial particles, X represents undetected final particles, n represents the quantum number of the heavy quarkonium under consideration, and the momentum p_H of the detected $\mu^+\mu^-$ pair fulfills the condition

$$p_H^2 \simeq M^2, \tag{69}$$

where M is the mass of the heavy quarkonium under consideration. According to the collinear factorization theorem presented in Refs. [24–28], we have

$$\begin{aligned}\sum_X \mathrm{d}\sigma_{A+B\to\mu^+\mu^-(n,p_H)+X} &= \sum_{i,X} \mathrm{d}\sigma_{A+B\to i+X} \otimes D_{i\to\mu^+\mu^-(n,p_H)} \\ &+ \sum_{\kappa,X} \mathrm{d}\sigma_{A+B\to Q\bar{Q}(\kappa)+X} \otimes D_{Q\bar{Q}(\kappa)\to\mu^+\mu^-(n,p_H)} \\ &+ \mathcal{O}(M^4/p_T^4) + \cdots,\end{aligned} \tag{70}$$

where $D_{i\to\mu^+\mu^-(n,p_H)}$ and $D_{Q\bar{Q}(\kappa)\to\mu^+\mu^-(n,p_H)}$ represent fragmentation functions for i and $Q\bar{Q}(\kappa)$ to the state $\mu^+\mu^-(n, p_H)$ under the evolution of QCD and QED interactions, and the ellipsis represents contributions of the process with the $\mu^+\mu^-$ pair produced in the short-distance (order $1/p_T$) subprocess.

It is convenient to consider fragmentation functions $D_{i\to\mu^+\mu^-(n,p_H)}$ and $D_{Q\bar{Q}(\kappa)\to\mu^+\mu^-(n,p_H)}$ in the rest frame of the $\mu^+\mu^-$ pair. The $\mu^+\mu^-$ pair can be produced in a direct short-distance process (order $1/M$) involving the states i or $Q\bar{Q}(\kappa)$. They can also be produced in an indirect short-distance process (order $1/M$) involving intermediate states with momenta squared of order M^2. We show examples of these two cases in Fig. 8.

Infrared divergences in fragmentation functions $D_{i\to\mu^+\mu^-(n,p_H)}$ and $D_{Q\bar{Q}(\kappa)\to\mu^+\mu^-(n,p_H)}$ are caused by (i) infrared gluons exchanged between final undetected particles, (ii) infrared gluons exchanged between final undetected particles and intermediate states that evolve to the $\mu^+\mu^-$ pair, (iii) infrared gluons exchanged between intermediate states that evolve to the $\mu^+\mu^-$ pair, and (iv) infrared QED interactions and possible interference terms.

We do not consider infrared QED interactions here, as such interactions are suppressed by the QED coupling constant. As in Refs. [22,23], we classify the QCD interactions into two types: the topologically factorized and topologically unfactorized interactions. Examples of these two types are shown in Fig. 9.

For the first diagram in Fig. 9, the infrared gluons do not produce pinch singular points unless the two intermediate quarks that annihilate to the $\mu^+\mu^-$ pair are at rest [30,31]. In this case, the effects of couplings between infrared gluons and intermediate quarks can be absorbed into two Wilson lines that lie along the same (time-like) direction. We notice that

$$Y^\dagger_{ij}(x)Y_{jk}(x) = \delta_{ik}, \qquad (Y)^\dagger_{ij}(x)Y_{ki}(x) = \delta_{jk} \tag{71}$$

for classical fields $A^\mu(x)$, where $Y_n(x)$ is the time-like Wilson line:

$$Y(x) = \mathcal{P}\exp\left(-ig\int_0^\infty \mathrm{d}sA^0(x^0 + s, \vec{x})\right). \tag{72}$$

To clarify the effects of self-energy graphs of the Wilson lines, we consider the diagram shown in Fig. 10. It can then be written as

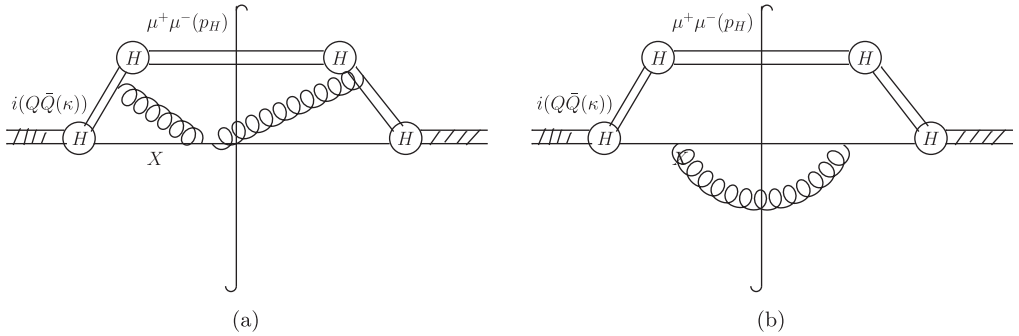

FIG. 9. (a) Example of topologically unfactorized QCD interactions. (b) Example of topologically factorized QCD interactions.

$$\Sigma_{10}^{\mu\nu}(x,y,\mathcal{O}(A)) \equiv \langle T\{\bar{\psi}Y^\dagger\gamma^\mu\mathcal{K}Y\psi(x)\mathcal{O}(A)\bar{\psi}Y^\dagger\gamma^\nu Y\psi(y)\}\rangle$$
$$\propto \int \mathcal{D}\psi(z)\mathcal{D}\bar{\psi}(z)\mathcal{D}A^\mu(z)\bar{\psi}Y^\dagger\gamma^\mu\mathcal{K}Y\psi(x)\bar{\psi}Y^\dagger\gamma^\nu Y\psi\mathcal{O}(A)e^{i\int \mathrm{d}^4z\mathcal{L}(\psi,A)(z)}, \tag{73}$$

where $\mathcal{K}=1$ for quarks produced as a color singlet and $\mathcal{K}=t^a$ for those produced as a color octet, $\bar{\psi}\gamma^\nu\psi$ is the electromagnetic current, $\mathcal{O}(A)$ represents operators at the other end of soft gluons of the type S_1, and the Lagrangian density $\mathcal{L}(\psi,A)(z)$ reads

$$\mathcal{L}(\psi,A)(z) = \bar{\psi}(i\not{\partial}-m)\psi(z) + \frac{1}{2g^2}\mathrm{tr}([\partial^\mu - igA^\mu,\partial^\nu - igA^\nu])^2(z). \tag{74}$$

We do not consider the effects of the gauge-fixing term and ghost fields for simplicity. We have

$$\Sigma_{10}^{\mu\nu}(x,y,\mathcal{O}(A)) = \frac{\langle T\{\bar{\psi}Y^\dagger\gamma^\mu Y\psi(x)\bar{\psi}Y^\dagger\gamma^\nu Y\psi(y)\}\rangle}{\int[\mathcal{D}\psi(z)][\mathcal{D}\bar{\psi}(z)][\mathcal{D}A^\mu(z)]\bar{\psi}\gamma^\mu\psi(x)\bar{\psi}\gamma^\nu\psi e^{i\int \mathrm{d}^4z\mathcal{L}(\psi,A)(z)}}$$
$$\times\int[\mathcal{D}\psi(z)][\mathcal{D}\bar{\psi}(z)][\mathcal{D}A^\mu(z)]\bar{\psi}\gamma^\mu\mathcal{K}\psi(x)\bar{\psi}\gamma^\nu\psi\mathcal{O}(A)e^{i\int \mathrm{d}^4z\mathcal{L}(\psi,A)(z)} \tag{75}$$

for quarks produced as a color singlet and

$$\Sigma_{10}^{\mu\nu}(x,y,\mathcal{O}(A)) = \frac{\langle T\{\bar{\psi}Y^\dagger\gamma^\mu t^a Y\psi(x)\bar{\psi}Y^\dagger\gamma^\nu Y\psi(y)\bar{\psi}t^a\psi(0)\}\rangle}{\int[\mathcal{D}\psi(z)][\mathcal{D}\bar{\psi}(z)][\mathcal{D}A^\mu(z)]\bar{\psi}Y^\dagger\gamma^\mu t^a Y\psi(x)\bar{\psi}Y^\dagger\gamma^\nu Y\psi(y)\bar{\psi}t^a\psi(0)e^{i\int \mathrm{d}^4z\mathcal{L}(\psi,A)(z)}}$$
$$\times\int[\mathcal{D}\psi(z)][\mathcal{D}\bar{\psi}(z)][\mathcal{D}A^\mu(z)]\bar{\psi}\gamma^\mu Y^\dagger t^a Y\psi(x)\bar{\psi}\gamma^\nu\psi\mathcal{O}^a(A)e^{i\int \mathrm{d}^4z\mathcal{L}(\psi,A)(z)} = 0. \tag{76}$$

We see that infrared divergences are topologically factorized in the color-singlet case and vanish in the color-octet case.

For the second diagram in Fig. 9, infrared divergences cancel out in the summation over all possible undetected states X.

There are, of course, more complicated diagrams that contribute to the fragmentation functions $D_{i\to\mu^+\mu^-(n,p_H)}$ and $D_{Q\bar{Q}(\kappa)\to\mu^+\mu^-(n,p_H)}$. For these diagrams, gluons that couple to nearly on-shell intermediate particles which connect two short-distance (order $1/M$) subdiagrams do not produce pinch singular points in the infrared region unless the relative velocities between these intermediate particles vanish [30,31]. In the case that these relative velocities do vanish, we can repeat the analysis for Fig. 10. We consider the matrix element

$$\langle X|T\{\mathcal{M}(Y_n\psi,Y_n\tilde{A}Y_n^\dagger)(y)\bar{\psi}\gamma^\mu\psi(x)\mathcal{O}(A)\}|0\rangle \propto \int_{(\psi(z),\bar{\psi}(z),\tilde{A}^\mu(z),A^\mu(z))|_{z^0\to\infty}=X}[\mathcal{D}\psi(z)][\mathcal{D}\bar{\psi}(z)][\mathcal{D}\tilde{A}^\mu(z)][\mathcal{D}A^\mu(z)]$$
$$\times\mathcal{M}(Y_n\psi,Y_n\tilde{A}Y_n^\dagger)(y)\bar{\psi}\gamma^\mu\psi(x)\mathcal{O}(A)e^{i\int \mathrm{d}^4z\mathcal{L}(\psi,\tilde{A},A)(z)} \tag{77}$$

with the proportional coefficient independent of the operator $\mathcal{O}(A)$, where X represents any possible final states, $\tilde{A}$ represents the field corresponding to gluons with finite momenta, Y_n is the Wilson line

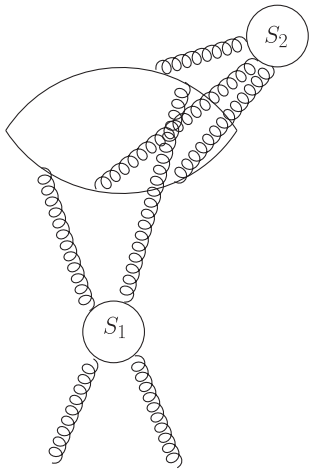

FIG. 10. Typical diagram that contributes to the infrared divergences of topologically unfactorized diagrams.

$$Y_n(x) = \mathcal{P}\exp\left(-ig\int_0^\infty \mathrm{d}s n\cdot A(x^\mu + n^\mu)\right) \quad (78)$$

with n^μ the direction vector along the motion of direction of the intermediate particles on the pinch surfaces, $\mathcal{M}(Y_n\psi, Y_n\tilde{A}Y_n^\dagger)$ represents effective operators that describe the interactions between infrared gluons and intermediate particles that connect two short-distance (order $1/M$) subdiagrams, $\mathcal{O}(A)$ represents operators that describe interactions between infrared gluons and the undetected particles X, and the Lagrangian density $\mathcal{L}(\psi, A)(z)$ reads

$$\begin{aligned}\mathcal{L}(\psi,\tilde{A},A)(z) &= \bar{\psi}(i\not{\partial} - m)\psi(z) \\ &\quad + \frac{1}{2g^2}\mathrm{tr}([\partial^\mu - ig\tilde{A}^\mu, \partial^\nu - ig\tilde{A}^\nu])^2(z) \\ &\quad + \frac{1}{2g^2}\mathrm{tr}([\partial^\mu - igA^\mu, \partial^\nu - igA^\nu])^2(z).\end{aligned} \quad (79)$$

We do not consider the effects of the gauge-fixing term and ghost fields for simplicity. It is convenient for us to make the relative velocities between the intermediate particles slightly deviate from 0 so that Coulomb divergences caused by the exchange of Coulomb gluons between these intermediate states (which do not affect the topological factorization) do not disturb us. We notice that

$$Y_n^\dagger Y_n = 1, \qquad Y_n t^a Y_n = Y_n^{ab} t^b. \quad (80)$$

Thus, topologically unfactorized infrared divergences are produced by the matrix element

$$\begin{aligned}S(0) &\equiv \sum_X \langle 0|\bar{T}\{\mathcal{M}^\dagger(\ldots, Y_n^{ij}(0),\ldots, Y_n^{ab}(0),\ldots)\mathcal{O}^\dagger(\ldots, Y_l(0),\ldots)\}|X\rangle \\ &\quad\times \langle X|T\{\mathcal{M}(\ldots, Y_n^{jk}(0),\ldots, Y_n^{bc}(0),\ldots)\mathcal{O}(\ldots, Y_l(0),\ldots)\}|0\rangle \\ &= \langle 0|\bar{T}\{\mathcal{M}^\dagger(\ldots, Y_n^{ij}(0),\ldots, Y_n^{ab}(0),\ldots)\mathcal{O}^\dagger(\ldots, Y_l(0),\ldots)\} \\ &\quad\times T\{\mathcal{M}(\ldots, Y_n^{jk}(0),\ldots, Y_n^{bc}(0),\ldots)\mathcal{O}(\ldots, Y_l(0),\ldots)\}|0\rangle.\end{aligned} \quad (81)$$

For the classical configurations $A^\mu(x)$, one can make use of unitarity to show that we can make the substitution

$$Y_n \to 1, \qquad Y_l \to 1 \quad (82)$$

in Eq. (81) without changing the matrix element.

For quantum operators $A^\mu(x)$, we consider the Wilson lines

$$W_n(0,s) \equiv \mathcal{P}\exp\left(-ig\int_0^s \mathrm{d}\lambda n\cdot A(\lambda n^\mu)\right), \quad (83)$$

$$W_l(0,s) \equiv \mathcal{P}\exp\left(-ig\int_0^s \mathrm{d}\lambda l\cdot A(\lambda l^\mu)\right). \quad (84)$$

One can easily see that

$$Y_n(0) = W_n(0,\infty), \qquad Y_l(0) = W_l(0,\infty). \quad (85)$$

We consider the matrix element

$$\begin{aligned}S(0,s) &\equiv \langle 0|\bar{T}\{\mathcal{M}^\dagger(\ldots, W_n^{ij}(0,s),\ldots, W_n^{ab}(0,s),\ldots) \\ &\quad\times \mathcal{O}^\dagger(\ldots, W_l(0,s),\ldots)\}T\{\mathcal{M}(\ldots, W_n^{jk}(0,s),\ldots, \\ &\quad\times W_n^{bc}(0,s),\ldots)\mathcal{O}(\ldots, W_l(0,s),\ldots)\}|0\rangle.\end{aligned} \quad (86)$$

We have

$$\begin{aligned}\frac{\mathrm{d}}{\mathrm{d}s}S(0,s) &= ig\langle 0|\bar{T}\{\mathcal{M}^{\dagger}(\ldots,W_n^{ij'}(0,s),\ldots,W_n^{ab}(0,s),\ldots)\mathcal{O}^{\dagger}(\ldots,W_l(0,s),\ldots)\}n\cdot A_{j'j}(sn^{\mu})\\ &\quad\times T\{\mathcal{M}(\ldots,W_n^{jk}(0,s),\ldots,W_n^{bc}(0,s),\ldots)\mathcal{O}(\ldots,W_l(0,s),\ldots)\}|0\rangle\\ &\quad- ig\langle 0|\bar{T}\{\mathcal{M}^{\dagger}(\ldots,W_n^{ij}(0,s),\ldots,W_n^{ab}(0,s),\ldots)\mathcal{O}^{\dagger}(\ldots,W_l(0,s),\ldots)\}\\ &\quad\times n\cdot A_{jj'}(sn^{\mu})T\{\mathcal{M}(\ldots,W_n^{j'k}(0,s),\ldots,W_n^{bc}(0,s),\ldots)\mathcal{O}(\ldots,W_l(0,s),\ldots)\}|0\rangle+\cdots\\ &= 0. \end{aligned} \tag{87}$$

We see that

$$S(0,s) = S(0,0). \tag{88}$$

In particular, we have

$$S(0) = S(0,\infty) = S(0,0) = S(0)|_{A^{\mu}=0}. \tag{89}$$

We conclude that topologically unfactorized infrared divergences cancel out.

We see that the fragmentation functions $D_{i\to\mu^+\mu^-(n,p_H)}$ and $D_{Q\bar{Q}(\kappa)\to\mu^+\mu^-(n,p_H)}$ are free from topologically unfactorized infrared divergences in the rest frame of the $\mu^+\mu^-$ pair. The detailed proof of this conclusion will be presented in other works. We then have

$$D_{i\to\mu^+\mu^-(n,p_H)} = D_{i\to\mu^+\mu^-(n,p_H)} - D^{\mathrm{div}}_{i\to\mu^+\mu^-(n,p_H)}, \tag{90}$$

$$D_{Q\bar{Q}(\kappa)\to\mu^+\mu^-(n,p_H)} = D_{Q\bar{Q}(\kappa)\to\mu^+\mu^-(n,p_H)} - D^{\mathrm{div}}_{Q\bar{Q}(\kappa)\to\mu^+\mu^-(n,p_H)}, \tag{91}$$

where $D^{\mathrm{div}}_{i\to\mu^+\mu^-(n,p_H)}$ and $D^{\mathrm{div}}_{Q\bar{Q}(\kappa)\to\mu^+\mu^-(n,p_H)}$ represent topologically unfactorized infrared divergences produced by various explicit diagrams in $D_{i\to\mu^+\mu^-(n,p_H)}$ and $D_{Q\bar{Q}(\kappa)\to\mu^+\mu^-(n,p_H)}$. We can then make the decomposition

$$\begin{aligned}D_{i\to\mu^+\mu^-(n,p_H)} &= D_{i\to H}\otimes d_{H\to\mu^+\mu^-(n,p_H)} - (D_{i\to H}\otimes d_{H\to\mu^+\mu^-(n,p_H)})^{\mathrm{div}} + D_{i\to\mu^+\mu^-(n,p_H)} - D_{i\to H}\otimes d_{H\to\mu^+\mu^-(n,p_H)}\\ &\quad - D^{\mathrm{div}}_{i\to\mu^+\mu^-(n,p_H)} + (D_{i\to H}\otimes d_{H\to\mu^+\mu^-(n,p_H)})^{\mathrm{div}}, \end{aligned} \tag{92}$$

$$\begin{aligned}D_{Q\bar{Q}(\kappa)\to\mu^+\mu^-(n,p_H)} &= D_{Q\bar{Q}(\kappa)\to H}\otimes d_{H\to\mu^+\mu^-(n,p_H)} - (D_{Q\bar{Q}(\kappa)\to H}\otimes d_{H\to\mu^+\mu^-(n,p_H)})^{\mathrm{div}} + D_{Q\bar{Q}(\kappa)\to\mu^+\mu^-(n,p_H)}\\ &\quad - D_{Q\bar{Q}(\kappa)\to H}\otimes d_{H\to\mu^+\mu^-(n,p_H)} - D^{\mathrm{div}}_{Q\bar{Q}(\kappa)\to\mu^+\mu^-(n,p_H)} + (D_{Q\bar{Q}(\kappa)\to H}\otimes d_{H\to\mu^+\mu^-(n,p_H)})^{\mathrm{div}}, \end{aligned} \tag{93}$$

where $d_{H\to\mu^+\mu^-(n,p_H)}$ represents the short-distance (order $1/m$) evolution of the heavy quarkonium H to the $\mu^+\mu^-$ pair, $D_{i\to H}$ and $D_{Q\bar{Q}(\kappa)\to H}$ represent the long-distance evolution of the parton i or the heavy quark pair $Q\bar{Q}$ to the hadron H under consideration, and $(D_{i\to H}\otimes d_{H\to\mu^+\mu^-(n,p_H)})^{\mathrm{div}}$ and $(D_{Q\bar{Q}(\kappa)\to H}\otimes d_{H\to\mu^+\mu^-(n,p_H)})^{\mathrm{div}}$ represent the infrared divergences of the functions $D_{i\to H}$ and $D_{Q\bar{Q}(\kappa)\to H}$. We have

$$\begin{aligned}&D_{i\to H}\otimes d_{H\to\mu^+\mu^-(n,p_H)} - (D_{i\to H}\otimes d_{H\to\mu^+\mu^-(n,p_H)})^{\mathrm{div}}\\ &\quad= (D_{i\to H} - D^{\mathrm{div}}_{i\to H})\otimes d_{H\to\mu^+\mu^-(n,p_H)}, \end{aligned} \tag{94}$$

$$\begin{aligned}&D_{Q\bar{Q}(\kappa)\to H}\otimes d_{H\to\mu^+\mu^-(n,p_H)} - (D_{Q\bar{Q}(\kappa)\to H}\otimes d_{H\to\mu^+\mu^-(n,p_H)})^{\mathrm{div}}\\ &\quad= (D_{Q\bar{Q}(\kappa)\to H} - D^{\mathrm{div}}_{Q\bar{Q}(\kappa)\to H})\otimes d_{H\to\mu^+\mu^-(n,p_H)}. \end{aligned} \tag{95}$$

Other terms in the fragmentation functions $D_{i\to\mu^+\mu^-(n,p_H)}$ and $D_{Q\bar{Q}(\kappa)\to\mu^+\mu^-(n,p_H)}$ are suppressed by the QED coupling constant α and the small decay width $\Gamma_H^{\mu^+\mu^-}$ of the heavy quarkonium H to the $\mu^+\mu^-$ pair. We thus have

$$\begin{aligned}D_{i\to\mu^+\mu^-(n,p_H)} &= (D_{i\to H} - D^{\mathrm{div}}_{i\to H})\otimes d_{H\to\mu^+\mu^-(n,p_H)}\\ &\quad\times(1 + O(\alpha) + O(\Gamma_H^{\mu^+\mu^-})), \end{aligned} \tag{96}$$

$$\begin{aligned}D_{Q\bar{Q}(\kappa)\to\mu^+\mu^-(n,p_H)} &= (D_{Q\bar{Q}(\kappa)\to H} - D^{\mathrm{div}}_{Q\bar{Q}(\kappa)\to H})\\ &\quad\otimes d_{H\to\mu^+\mu^-(n,p_H)}\\ &\quad\times(1 + O(\alpha) + O(\Gamma_H^{\mu^+\mu^-})). \end{aligned} \tag{97}$$

It is interesting to mention that intermediate sates which connect two short-distance (order $1/M$) subdiagrams do not produce infrared divergence terms unless the relative velocities of these states vanish. Thus such infrared divergences occur only when the momentum of the final $\mu^+\mu^-$ pair p_H takes some special values. Such infrared divergences vanish in the integral of p_H once infrared

divergences are no worse than logarithms. For the cancellation of topologically unfactorized divergences, however, the integral over p_H is not necessary.

VI. CONCLUSION

We presented a scheme to cancel out topologically unfactorized infrared divergences in inclusive productions of heavy quarkonia. In Ref. [5], it was proposed that such divergences do cancel out according to the KLN cancellation [32,33] once the summation over the undetected particles is made. However, the explicit calculations at NNLO in Refs. [22,23] showed that the summation is not inclusive enough to cancel out topologically unfactorized infrared divergences.

In Refs. [22,23], the final states were chosen as color-singlet heavy quark pair plus any other states with the final heavy quark and heavy antiquark both on shell. We notice that the color-singlet heavy quark pair is not invariant under the evolution of infrared QCD interactions. In particular, color states of the heavy quark pair may change to others under this evolution. Thus the KLN cancellation—for which the summation over all states that arise from such evolution is necessary—do not work simply. In fact, practical heavy quarkonia is not the color-singlet heavy quark pair. It seems plausible to define heavy quarkonia as resonance states which are invariant under the evolution of infrared QCD interactions, as we do for the J/ψ particle. Thus summation over higher Fock states is necessary. Such a summation, however, does not make topologically unfactorized infrared divergences disappear, as shown in our calculations.

It is interesting to point out that the states HX do not form the invariant subspace of the evolution of infrared QCD interactions even if the detected particle H is itself invariant under this evolution. Exchanges of soft gluons between H and X may change the state H; for example, they may cause the transition between heavy quarkonia. Such a transition may exist even if all soft gluons are infrared! We notice that heavy quarkonia are reconstructed from their decay products in practical experiments. Final decay products like $\mu^+\mu^-$ (the invariant mass of which is required to be near the mass of the detected heavy quarkonium H) can be produced by the decay of H and other possible states. Thus the practical process is indeed inclusive regarding the states arising from the evolution of infrared QCD interactions. In this paper, we have shown that topologically unfactorized infrared divergences do cancel out in the fragmentation functions $D_{i\to\mu^+\mu^-(n,p_H)}$ and $D_{Q\bar{Q}(\kappa)\to\mu^+\mu^-(n,p_H)}$!

It seems more reasonable to consider the NRQCD factorization for the fragmentation functions $D_{i\to\mu^+\mu^-(n,p_H)}$ and $D_{Q\bar{Q}(\kappa)\to\mu^+\mu^-(n,p_H)}$, as they are free from topologically unfactorized infrared divergences. If the NRQCD factorization theorem holds for these fragmentation functions, then we have

$$\begin{aligned} D_{i\to\mu^+\mu^-(n,p_H)} = \sum_n & (d_{i\to Q\bar{Q}(n)} - d^{\rm div}_{i\to Q\bar{Q}(n)}) \\ & \times (\langle\mathcal{O}^H(n)\rangle - \langle\mathcal{O}^H(n)\rangle^{\rm div}) \\ & \otimes (d_{H\to\mu^+\mu^-(n,p_H)} - d^{\rm div}_{H\to\mu^+\mu^-(n,p_H)}) \\ & \times (1 + O(\alpha) + O(\Gamma_H^{\mu^+\mu^-})), \end{aligned} \tag{98}$$

$$\begin{aligned} D_{Q\bar{Q}(\kappa)\to\mu^+\mu^-(n,p_H)} = \sum_n & (d_{Q\bar{Q}(\kappa)\to Q\bar{Q}(n)} - d^{\rm div}_{Q\bar{Q}(\kappa)\to Q\bar{Q}(n)}) \\ & \times (\langle\mathcal{O}^H(n)\rangle - \langle\mathcal{O}^H(n)\rangle^{\rm div}) \\ & \otimes (d_{H\to\mu^+\mu^-(n,p_H)} - d^{\rm div}_{H\to\mu^+\mu^-(n,p_H)}) \\ & \times (1 + O(\alpha) + O(\Gamma_H^{\mu^+\mu^-})). \end{aligned} \tag{99}$$

We do not require that the matrix elements $\langle\mathcal{O}^H(n)\rangle$ absorb all infrared divergences in the fragmentation functions $D_{i\to H}$ and $D_{Q\bar{Q}(\kappa)\to H}$. Generally speaking, parts of infrared divergences in the functions $D_{i\to H}$ and $D_{Q\bar{Q}(\kappa)\to H}$ are canceled by infrared divergences of other terms in the fragmentation functions $D_{i\to\mu^+\mu^-(n,p_H)}$ and $D_{Q\bar{Q}(\kappa)\to\mu^+\mu^-(n,p_H)}$. We thus have obtained a NRQCD factorization theorem for the inclusive production of the heavy quarkonium H once the NRQCD factorization for the fragmentation functions $D_{i\to\mu^+\mu^-(n,p_H)}$ and $D_{Q\bar{Q}(\kappa)\to\mu^+\mu^-(n,p_H)}$ holds.

ACKNOWLEDGMENTS

The author thanks Y. Q. Chen for helpful discussions and important suggestions about the work.

[1] N. Brambilla *et al.*, Eur. Phys. J. C **71**, 1534 (2011).
[2] G. T. Bodwin, E. Braaten, E. Eichten, S. L. Olsen, and T. K. Pedlar, arXiv:1307.7425.
[3] C. Quigg and J. L. Rosner, Phys. Rep. **56**, 167 (1979).
[4] W. Caswell and G. Lepage, Phys. Lett. B **167**, 437 (1986).
[5] G. T. Bodwin, E. Braaten, and G. P. Lepage, Phys. Rev. D **D51**, 1125 (1995)**D55**, 5853(E) (1997).
[6] E. Braaten and S. Fleming, Phys. Rev. Lett. **74**, 3327 (1995).
[7] P. L. Cho and A. K. Leibovich, Phys. Rev. D **53**, 150 (1996).

[8] P. L. Cho and A. K. Leibovich, Phys. Rev. D **53**, 6203 (1996).
[9] J. Amundson, S. Fleming, and I. Maksymyk, Phys. Rev. D **56**, 5844 (1997).
[10] M. Beneke and M. Krämer, Phys. Rev. D **55**, R5269 (1997).
[11] E. Braaten and Y.-Q. Chen, Phys. Rev. D **54**, 3216 (1996).
[12] M. Cacciari and M. Krämer, Phys. Rev. Lett. **76**, 4128 (1996).
[13] H.-W. Huang and K.-T. Chao, Phys. Rev. D **54**, 6850 (1996); **56**, 1821(E) (1997).
[14] E. Braaten, B. A. Kniehl, and J. Lee, Phys. Rev. D **62**, 094005 (2000).
[15] E. Braaten, S. Fleming, and A. K. Leibovich, Phys. Rev. D **63**, 094006 (2001).
[16] B. Gong and J.-X. Wang, Phys. Rev. D **77**, 054028 (2008).
[17] Y.-Q. Ma, K. Wang, and K.-T. Chao, Phys. Rev. Lett. **106**, 042002 (2011).
[18] M. Butenschoen and B. A. Kniehl, Phys. Rev. D **84**, 051501 (2011).
[19] B. Gong, L.-P. Wan, J.-X. Wang, and H.-F. Zhang, Phys. Rev. Lett. **112**, 032001 (2014).
[20] G. T. Bodwin, X. Garcia i Tormo, and J. Lee, Phys. Rev. Lett. **101**, 102002 (2008).
[21] G. T. Bodwin, X. Garcia i Tormo, and J. Lee, Phys. Rev. D **81**, 114014 (2010).
[22] G. C. Nayak, J. W. Qiu, and G. F. Sterman, Phys. Rev. D **72**, 114012 (2005).
[23] G. C. Nayak, J.-W. Qiu, and G. F. Sterman, Phys. Rev. D **74**, 074007 (2006).
[24] Z.-B. Kang, J.-W. Qiu, and G. Sterman, Phys. Rev. Lett. **108**, 102002 (2012).
[25] Z.-B. Kang, J.-W. Qiu, and G. Sterman, Nucl. Phys. B, Proc. Suppl. **214**, 39 (2011).
[26] Z.-B. Kang, Y.-Q. Ma, J.-W. Qiu, and G. Sterman, Phys. Rev. D **90**, 034006 (2014).
[27] S. Fleming, A. K. Leibovich, T. Mehen, and I. Z. Rothstein, Phys. Rev. D **86**, 094012 (2012).
[28] S. Fleming, A. K. Leibovich, T. Mehen, and I. Z. Rothstein, Phys. Rev. D **87**, 074022 (2013).
[29] J. C. Collins and D. E. Soper, Nucl. Phys. **B194**, 445 (1982).
[30] S. Coleman and R. E. Norton, Nuovo Cimento **38**, 438 (1965).
[31] G. Sterman, *An Introduction to Quantum Field theory* (Cambridge University Press, Cambridge, England, 1993).
[32] T. Kinoshita, J. Math. Phys. (N.Y.) **3**, 650 (1962).
[33] T. D. Lee and M. Nauenberg, Phys. Rev. **133**, B1549 (1964).